

# Phase Retrieval of Vortices in Bose-Einstein Condensates

Ron Ziv<sup>1</sup>, Anatoly Patsyk<sup>2</sup>, Yaakov Lumer<sup>2</sup>, Yoav Sagi<sup>2</sup>, Yonina C. Eldar<sup>3</sup>  
and Mordechai Segev<sup>1,2</sup>

<sup>1</sup> Department of Electrical Engineering, Technion, Haifa 3200003, Israel

<sup>2</sup> Department of Physics and Solid State Institute, Technion, Haifa 3200003, Israel

<sup>3</sup> Department of Mathematics and Computer Science, Weizmann Institute of Science, Rehovot 7610001, Israel

E-mail: ronziv@campus.technion.ac.il

## Abstract

We propose and demonstrate numerically a measurement scheme for complete reconstruction of the quantum wavefunctions of Bose-Einstein condensates, amplitude and phase, from a time of flight measurement. We identify a fundamental ambiguity present in the measurement of vortices and show how to overcome it by augmenting the measurement to allow reconstruction of matter-wave vortices and arrays of vortices.

---

## 1 Introduction

Bose-Einstein condensation (BEC) is a quantum state of matter where particles are trapped and cooled until they form a macroscopic population in a single quantum wavefunction. The theory[1] predicting this state waited 70 years to be validated and measured in the lab[2, 3] and since then has spun almost three decades of fruitful research in the field of ultra-cold atoms[4]. Yet, despite the progress, the commonly used measurement techniques of BECs are incomplete in the information they provide.

BECs are quantum objects, and as such they are matter waves, characterized by both amplitude and phase. Thus, to characterize a BEC, it is essential to obtain the complete map of their amplitude and phase everywhere in space, as they evolve. Direct mapping of this kind is currently beyond the experimental reach. Instead, current measurement techniques rely on imaging, where one shines light through the BEC cloud and records the shadow it casts on screen. This technique is inherently destructive: the radiation is absorbed by the atoms and heats the cloud. Two imaging modes are usually available: *in-situ* – mapping the density of particles inside the trap, or in the “far-field” by opening the trap and recording the density of particles after expansion of the cloud. This “far-field” measurement is termed time-of-flight (TOF)[5]. In these measurements, from the shadow cast by the particle cloud one can extract the atomic density. For the *in-situ* measurement this corresponds to the density of the trapped gas. If the particles do not interact with one another during the expansion, and if the initial size of the cloud is negligible relative to the final expanded size, then the TOF measurement provides the momentum distribution of the atomic cloud. In this case, the TOF measurement gives the “power spectrum” of the wavefunction, that is, the absolute value squared of the spatial Fourier transform of the wavefunction. If interactions are present during the expansion but the final density is low enough such that they become negligible, the kinetic energy of the measured momentum distribution reflects the initial kinetic plus interaction energy.

Somewhat similar to the measurements of optical beams, these measurements measure the magnitude of the density. Yet, as a BEC is a pure quantum state, it also has a well-defined phase structure[6] that cannot be obtained by these measurements alone. Thus, to recover the phase structure of the BEC wavefunction, interference measurements can be explored – either between different sections of the same BEC [7] or between different BECs [8]. However, interference measurements of cold atoms present experimental challenges[9], such as coherently splitting and recombining a BEC. Keeping in mind that the measurements are destructive and repeated measurements are fundamentally required because observables in quantum

mechanics are described by expectation values, exemplifies the difficulty of such atom interference experiments. Altogether, as interference measurements with BECs require precise and intricate control of the cloud, they are rarely used. This raises a natural question: Can the phase structure of a BEC be recovered without atomic interference[10]? This question is related to the well-known phase retrieval problem from optics, but with some important differences.

Traditionally, the phase retrieval problem is defined as the recovery of an object, amplitude and phase, from the magnitude of its Fourier transform [11]. This problem arises naturally in optical imaging as the far-field of an object (or the field at the focal plane of a lens) is proportional to the Fourier transform of the object that one wishes to image. As detectors (or a camera) only measure the field's intensity, the information measured is the magnitude (squared) of the Fourier transform, losing the phase information. Since the phase structure of a coherent light beam is also embedded in the far-field diffraction pattern, one can try and recover it computationally from the intensity measurement in the far-field. Surprisingly, by utilizing some elementary prior knowledge about the state to reconstruct (such as the "support" - the region within which the image resides) of 2D objects, one can often recover the phase in an iterative fashion for example by using Fienup's algorithm[12] from the late seventies,. Moreover, under sufficient conditions on the image, a unique solution can sometimes be guaranteed[13]. Additional prior knowledge, such as sparsity, can result in improvements in terms of the number of sample points (resolution of the detector), noise robustness and convergence rate of the algorithm, even of 1D objects, as was explored in many works[14–17]. In recent years, the problem has been studied extensively, and several measurement schemes and recovery algorithms have been proposed and demonstrated, facilitating recovery of the phase from various forms of generalized Fourier measurements [18–21].

The setting of phase-retrieval in optical imaging is very similar to TOF in BEC measurements, as the information of the initial state is embedded in some "far-field" plane. By the same logic, if the initial quantum state of the BEC includes a phase structure, it affects the evolution to the plane where TOF measurements are carried out; hence one can try and extract it from the TOF measurements. However, unlike the traditional phase retrieval problem from optics, where the relation between the electromagnetic field in the image plane and the field in the far-field is a simple Fourier transform, in BECs the relation is more complicated. Specifically, the particles constituting the BEC interact with one another; hence the propagation from the BEC to the measurement plane is no longer ballistic: it does not follow a simple linear relation (such as a Fourier transform) but instead is governed by a nonlinear evolution equation. Also, as noted, BEC measurements are inherently destructive, and BECs have a limited time within which they still act as a coherent entity when the trap is removed, which makes interference measurements very difficult.

The concept of phase retrieval has been proposed for BEC TOF measurements before [22], [23]. However, these methods do not handle well complex phase structures such as vortices, that naturally create ambiguities in a phase retrieval process based on density TOF measurements due to symmetries in propagation. These ambiguities cannot be resolved by a phase-retrieval algorithm. For example, employing the Fienup phase-retrieval methodology or a more modern technique [11] cannot reveal the rotation direction of a vortex such as in [24], or an array of vortices, as has been often studied in BECs [25], [26]. The issue of unravelling the directionality of vortices imprinted on the quantum wavefunctions of BECs is extremely important and interesting: they inherently possess a quantum number (the topological charge) and contain information about multiple phenomena such as phase-transitions (e.g., the Berezinskii-Kosterlitz-Thouless phase-transition [26] where pairs of counter-rotating vortices appear spontaneously), superfluid dynamics of the BEC[27], can be used to carry quantum information[28], and in vortex-solitons[29], [30] (Generally, phase plays an important role in solitons[31], [32]). Hence, the recovery of vortices in BECs is crucial and has many far-reaching implications for basic and applied science alike. However, all methods proposed thus far, with either linear or nonlinear evolution, are not suitable for reconstructing vortex states since the symmetries of the evolution equation prohibit any signature of the vortex orientation in the TOF density. **Namely, the magnitude measurement does not encode information on the order and sign of the vortex charge.** In the language of information processing, vortices can manifest non-trivial ambiguities in Fourier-type amplitude measurement, and the traditional phase-retrieval methodology is not able to reconstruct them, even when it is adapted to nonlinear evolution.

*Here, we propose and demonstrate in numerical simulations a simple scheme for the complete characterization of the quantum wavefunction of a Bose-Einstein condensation from TOF measurements, including wavefunctions containing vortices.* Our proposed measurement scheme is based on a simple variation to TOF measurements and does not require any kind of interference. The variation breaks the radial symmetry in the propagation, which is what causes the ambiguities in the measurement of vortices, and otherwise cannot be lifted by any algorithm. Our measurement scheme can resolve these ambiguities and facilitates the recovery of single vortices and of vortex arrays, including their directionality, which are highly difficult tasks that have thus far not been demonstrated without atomic interference or multiple measurement planes. Additionally, since the evolution of BECs is nonlinear, described by the Gross-Pitaevskii equation (GPE), our algorithm is based on nonlinear dynamical evolution rather than on the simple Fourier transform used in linear phase-retrieval problems.

## 2 Background

### 2.1 Mean field description

The object we wish to reconstruct is the wave function of a Bose-Einstein Condensate. The dynamics of the state of  $N$  particles are given by the many-body Hamiltonian. Under appropriate conditions, a mean-field approximation is valid, and the many-body Hamiltonian describing the ensemble of particles is reduced to the Gross-Pitaevskii equation[33], which is functionally equal to the non-linear Schrodinger-type equation:

$$\left( -\frac{\hbar^2}{2m} \nabla^2 + V(\mathbf{r}) + U_0 |\psi(\mathbf{r}, t)|^2 \right) \psi(\mathbf{r}, t) = i\hbar \partial_t \psi(\mathbf{r}, t) \quad (1)$$

where  $V(\mathbf{r})$  is the confining potential of the trap as a function of coordinate  $\mathbf{r}$ ,  $V$  typically being a real function, and  $U_0 > 0$  is the nonlinear coefficient that represents repulsion between particles due to interactions. Usually, it is reasonable to assume that the wavefunction is initially localized by the confining potential; hence knowledge of the region within which the wavefunction is nonzero (the "support") is tight.

An alternative mathematical description of the state above highlights the relation between the phase of the wavefunction and the flow of quantum gas. Through a hydrodynamics description[34], one can show that the following holds:

$$\begin{aligned} \psi(\mathbf{r}, \theta) &= f(\mathbf{r}, \theta) e^{i\phi(\mathbf{r}, \theta)} \\ \mathbf{v} &= \frac{\hbar}{m} \nabla \phi \end{aligned} \quad (2)$$

where  $\psi(\mathbf{r}, \theta)$  is the wavefunction describing the condensate in terms of its amplitude and phase and  $\mathbf{v}$  is the velocity of the condensate. One special type of flow (or phase pattern) is that of a vortex, that is, a field that circulates around a point. Mathematically it is described by a phase function of the functional form  $\phi(\mathbf{r}, \theta) = n\theta$ , where  $n$  is an integer because the phase modulus  $2\pi$  must be continuous. As a result, the rotation speed of vortices is always quantized in a quantum gas. Due to this quantization, one can assign a topological quantity to the wavefunction, the topological charge,  $n$  in our case. In a similar fashion, optical vortex beams are electromagnetic waves that carry orbital angular momentum (OAM), where  $n$  is the order of the OAM and its sign gives its direction.

### 2.2 Time of Flight measurement

A time-of-flight measurement is performed by opening the trap confining the condensate and allowing the atomic cloud to expand freely. After some propagation time, collimated light is launched through the cloud, the light is partially absorbed, and the shadow the atoms cast is recorded. The absorption coefficient is proportional to the density of atoms. Mathematically, this procedure translates to measuring  $|\psi(\mathbf{r}, t)|^2$  at some time  $T$  after the trap is removed and the atomic cloud is allowed to evolve freely, i.e., with no potential present, setting  $V(\mathbf{r})$  to zero in Eq. 1.

An important observation is that, when the trap is turned off, the potential-free Hamiltonian conserves orbital angular momentum and hence also conserves the total OAM of the state, even for the nonlinear evolution of the GPE. In the context of BECs containing vortices, this implies that the condensate conserves OAM in the free propagation of the TOF measurement. As the phase of a vortex is singular at its core, it manifests a zero density there. Due to the symmetries in Eq. 1, this zero density core persists throughout the propagation and hence is also present in the TOF measurement. This implies that the presence of a vortex can be detected by locating the zero density point. Alas, as the OAM is manifested in the phase of the state, it means that a state with opposite vortex direction results in identical density measurement; this means one cannot distinguish the directionality of the vortex flow from this measurement, as can be seen in Fig 1. Likewise, in a BEC with multiple vortices, locating the zero-density points does not reveal the rotation directions of the individual vortices. This fact presents a problem for the phase retrieval algorithm. For any reconstruction algorithm, when one measurement corresponds to two (or more) different inputs - the reconstruction problem is ill-posed and contains an ambiguity preventing recovery of the original input. While some ambiguities are trivial and not important, such as global phase, this type of ambiguity has a physical meaning, and hence lifting it is crucial for successful operation.

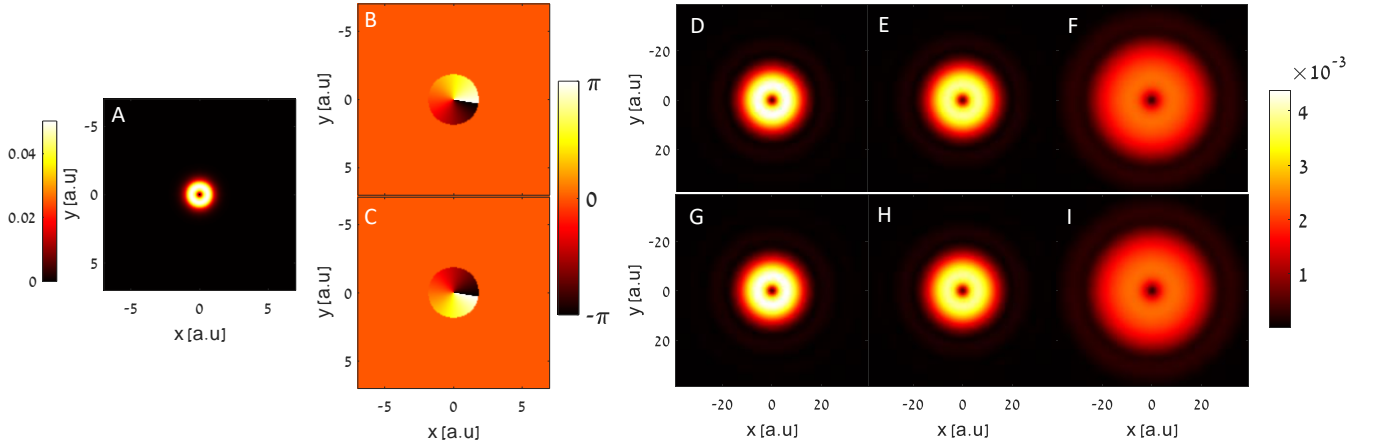


**Fig 1.** (A) Amplitude distribution of single  $m = \pm 1$  vortex state in arbitrary unit. (B) phase structure of vortex state  $m = 1$ . (C) phase structure of vortex state  $m = -1$ . (D-I) Top row: TOF measurement of state (B) with linear(D), weak(E) and strong nonlinear(F) propagation. Bottom row: TOF measurement for state (C) with linear,  $U_0 = 0$ , (G), weak,  $U_0 = 10^2$ , (H) and strong nonlinear,  $U_0 = 10^5$ , (I) propagation. See appendix B for simulation details.

### 2.3 Phase Retrieval

Phase retrieval is the mathematical problem of reconstructing a function from the magnitude of its Fourier transform. Of course, the Fourier transform has an inverse transform that can be utilized, but without the phase of the Fourier components - information is lost[35], and the transform is not bijective. Hence, recovering the initial object amounts to retrieving the phase in the Fourier plane. The phase retrieval problem has been studied extensively in the past and in recent years as well, bringing forth theoretical results guaranteeing uniqueness and stability under various prior constraints on the input and new classes of measurements [13] along with new algorithms for reconstruction[14, 32].

The most common phase retrieval algorithms are iterative, and are derived either by solving an underlying optimization problem, or by using alternating projections based on the following working principle: As we have two relevant planes, the object plane and the Fourier plane, one can impose the information one has at each plane and iterate between the two planes. For instance, one starts by drawing a random initial wavefunction guess and propagate it by Fourier transform to the far-field. Here, the magnitude is replaced with the measured Fourier magnitude. The field is then propagated back (inverse Fourier transform) to the object plane, where constraints are imposed, such as support, sparsity and more.

Traditional phase retrieval method, as noted above, were developed and used based on Fourier propagation. However, TOF measurements of BECs follow Eq. 1, which is nonlinear, and the measurements are not of the Fourier-transform squared. Rather, the measurements are taken over the atom density  $|\psi(\mathbf{r}, t)|^2$  some time  $t$  after the trap is removed.

Nevertheless, the underlying principle of these algorithms can still be applied to different mechanisms of evolution, linear or even nonlinear, as we show below. This idea has been proposed before in nonlinear optics [37] and also for BECs [22], but has thus far never been demonstrated experimentally with cold atoms. However, while these methods can work well, for measurements with ambiguities associated with the inherent symmetries of the evolution according to the GPE, Eq. 1 they can fail. In what follows, we describe our methodology of phase-retrieval of BECs, focusing on changing the measurement scheme for the challenging task of phase-retrieval of wavefunctions containing vortices.

## 3 Method

### 3.1 Augmented TOF

The reason an ambiguity arises in the measurement of the TOF images from vortices is time-reversal symmetry of the GPE, which transforms a right-handed vortex into a left-handed one, and vice versa. Thus, in order to alleviate this ambiguity, we propose to break explicitly this symmetry in the TOF propagation. We achieve this by a simple and easily implemented adaption to the TOF measurement. Instead of opening the BEC trap in the x-y axes simultaneously, we open the

trap in succession: one axis first and after sufficient evolution, the second axis. That is, there are two times relevant for propagation,  $T_1$  the propagation time under a partial potential active in one axis only, followed by free propagation for a time  $T_2$ , and then performing the measurement which yields the density of atoms. This procedure makes the Hamiltonian after releasing the atoms time-dependent and removes the time-reversal symmetry between positive and negative charge vortices. Here,  $T_2$  should be long enough such that the dynamics create enough mixing of phase information within this time interval. This is in analogy to the regular Fourier propagation, where one wants sufficient propagation to approximate the Fourier transform. Henceforth we refer to this methodology as augmented TOF. Our augmented TOF phase-retrieval methodology is conceptually similar to breaking the propagation symmetry in linear optics by an intermediate cylindrical lens [38].

Figure 2 shows the same states from Fig 1 after augmented TOF measurements, instead of the standard TOF measurements shown in Fig. 1. As shown in Fig. 2, unlike the regular TOF measurement that yields the same result for vortex of order 1 and -1 (Fig. 1), the augmented TOF produces different patterns regardless of the interaction strength.

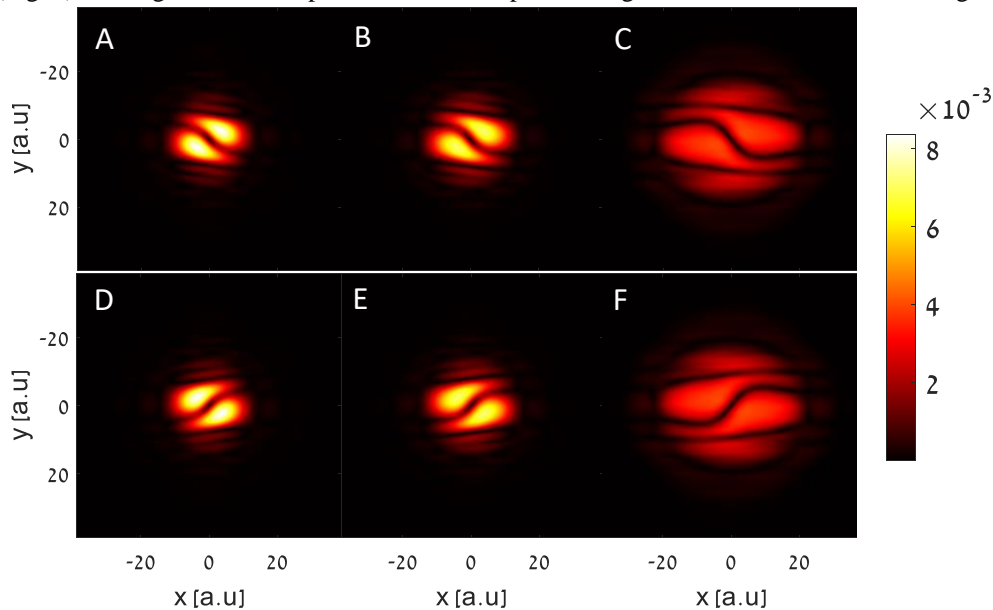


**Fig 2.** Top row: Augmented TOF measurement for vortex states of  $m=1$  with linear(A), weak(B) and strong nonlinear(C) propagation. Bottom row: Augmented TOF measurement for vortex states of  $m=-1$  with the same propagation parameters for linear(D), weak(E) and strong nonlinear(F) propagation.

### 3.2 GPE-Phase Retrieval Algorithm

We first address the phase retrieval problem for the nonlinear propagation represented by the GPE. The problem is similar to the common phase retrieval. Thus, the algorithm for this nonlinear evolution can be almost identical to common phase retrieval algorithms, with appropriate modification. As the propagation is no longer linear, we modify existing algorithms by replacing the Fourier propagation with GPE-based propagation, where we include in this propagation the different times under the partial trapping and free expansion. This is done by numerically solving the GPE for each iteration backward and forward. In principle, for methods requiring gradient computations, we would need to adapt the gradient as well. Instead, we focus on Fienup-type methods which rely on projections between planes so that we only modify the forward model while the rest of the algorithm steps remain unchanged. Our numerical solver is the split-step method or Beam Propagation Model[39]. As in-situ atom-density measurements are available for the BEC (sometimes at low resolution), we impose a magnitude constraint instead of support constraint in the in-situ plane. This scheme is sketched in Fig 3, where  $\psi_i$  is the wavefunction estimated at the trap plane in iteration  $i$  and  $\tilde{\psi}_i$  is the wavefunction estimate at the measurement plane, while wavefunctions without iteration index correspond to the measured images at each plane. Reconstruction results for this algorithm are presented in Section 4.2. The algorithm in Fig 3 is the same for the case of the BEC with our proposed augmented TOF measurement. The only difference is that the GPE propagation (and inverse) is done in two steps, numerical propagation

under the partial potential for a time  $T_1$  followed by numerical free propagation with no potential for a time  $T_2$ . The measurement constraint is changed into the augmented TOF instead of TOF.

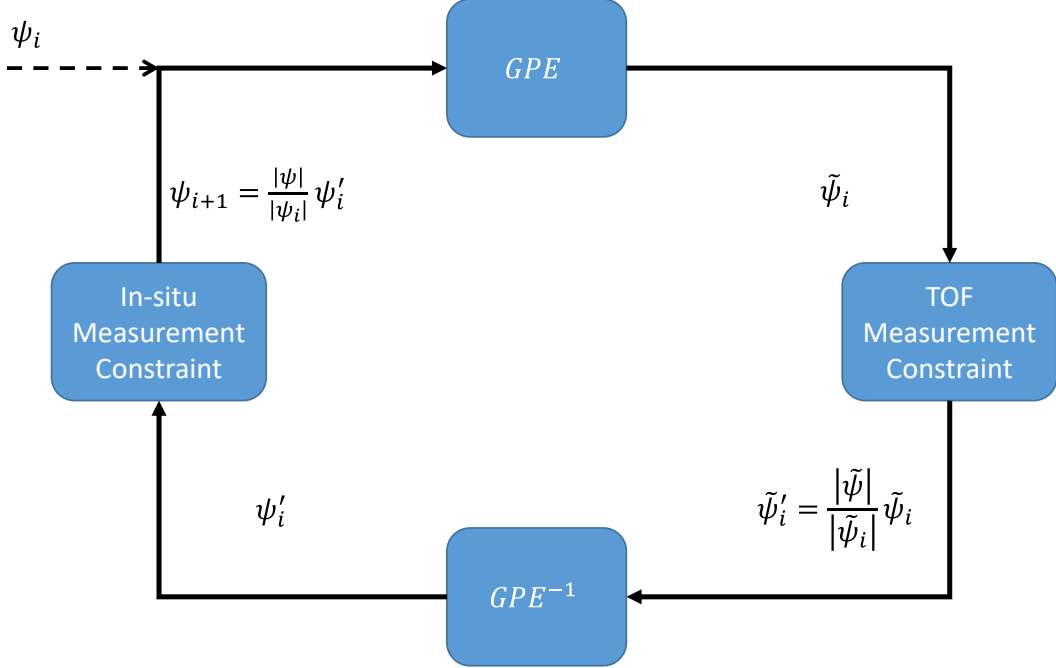


**Fig 3.** Graphical depiction of the iterative phase retrieval algorithm for the augmented TOF measurements of BEC.

### 3.3 $T_1$ Propagation Time

As the augmented TOF scheme introduces an extra parameter, the time under the partial trap, an immediate question arises: what is the optimal propagation time under the partial trap? to select a possible  $T_1$ , we choose to optimize the maximal norm difference between a vortex state of order 1 and order -1. That is:

$$\max_{T_1} \left\| \left| \psi_1(x, y, T_1 + T_2) \right|^2 - \left| \psi_{-1}(x, y, T_1 + T_2) \right|^2 \right\|_2^2 \quad (3)$$

where  $\psi_{\pm 1}(x, y, T_1 + T_2)$  is a vortex state with an order of  $\pm 1$ , as a function of propagation time under the partial trap  $T_1$ , followed by free propagation of a time  $T_2$ . The intuition behind this selection is maximizing the difference between the measured images in the augmented TOF for the ambiguous condensates.

We relax the above problem by solving for the linear regime of the GPE and taking  $T_2$  such that a far-field approximation is valid. Under these conditions, we show (Supp A.) that the norm difference is approximately proportional to:

$$\left\| \left| \psi_1(x, y, T_1 + T_2) \right|^2 - \left| \psi_{-1}(x, y, T_1 + T_2) \right|^2 \right\|_2^2 \propto \frac{1}{\sqrt{T_2(T_1 + T_2)}} \left| \sin\left(\frac{\Delta E T_1}{\hbar}\right) \right| \quad (4)$$

where  $\Delta E$  is the energy difference between the first and second modes of the trap. Hence, by setting  $\frac{\Delta E T_1}{\hbar} = \pi/2$  we can expect a maximal difference between the two states. We validate this result numerically, as shown in Fig. 4. We note that this result can be computed directly from the parameters of the system, with no additional measurement required for the calculation.

In general, these results can be further developed to deal with high-order vortices and more intricate phase structures, such as lattice of vortices, and to optimize over the reconstruction error of the algorithm rather than the measurement difference. We leave these improvements for future works.

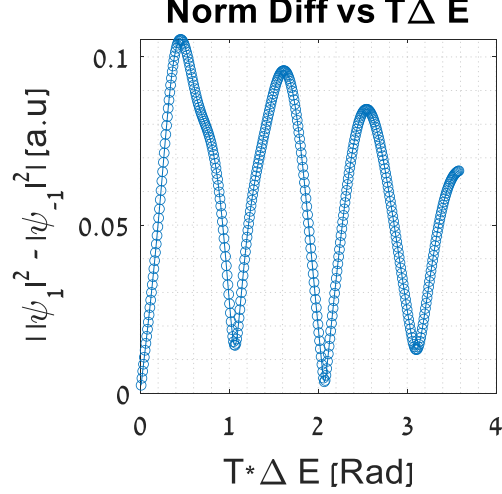


**Fig 4.** Norm difference between augmented TOF measurements of vortex states  $m = 1$  and  $m = -1$  as a function of propagation time  $T$ . Time axis is scaled by the energy difference between the second and first modes of the trap.

### 3.4 Reconstruction of a Lattice of Vortices

To test the proposed method, we simulate a more complex class of wavefunctions and show their respective reconstructions. As an example, we consider a  $3 \times 3$  lattice of order-one vortices. Each vortex having a random order sign and relative phase to the others. Each vortex by itself is a stationary order-one vortex state of the GPE equation with a single site potential well. We test the performance of our method on an ensemble of 150 such lattices. We measure the augmented time of flight and in-situ measurements for 150 wavefunctions and different interaction strengths and reconstruct the wavefunction based on the algorithm described in Section 4.1. Unlike the case of the single vortex state, where we analytically show there is an ambiguity in the TOF measurement, for the lattice case this is not that simple as only the total topological charge is conserved, yet single vortices can still split and merge during propagation hence local charge is not conserved. However, our numerical study reveals ambiguity also in the lattice case. This can be seen in Fig 5, where we attempt to reconstruct an initial wavefunction based on TOF and augmented TOF measurement. As shown there, for the TOF case, the algorithm converges into an erroneous phase signal, yet as shown in the figure, the augmented TOF yields the correct reconstructed wavefunction. These numerical experiments lead us to conjecture that some vortex lattices contain ambiguities in TOF measurements of BECs, which can be overcome by the new methodology of augmented TOF measurements and the accompanying algorithm. In order to test the reconstruction further, we simulate measurements in the presence of white gaussian noise of a varying degree of SNR ( $[60dB - 0dB]$ ), for an ensemble of 10 random vortex lattices similar to those in the previous test. While more tests are required to validate noise robustness, we numerically observe that we are able to reconstruct vortex lattices even in presence of high noise, as can be seen in Fig 6. Note that, while some noise is still present in the final phase reconstructed, it is located in regions of low magnitude (i.e., low signal strength) and that the direction of each vortex and its relative phase with respect to others can be easily distinguished. Remarkably, the final reconstructed augmented TOF measurement shows considerable noise reduction, thereby indicating good performance.

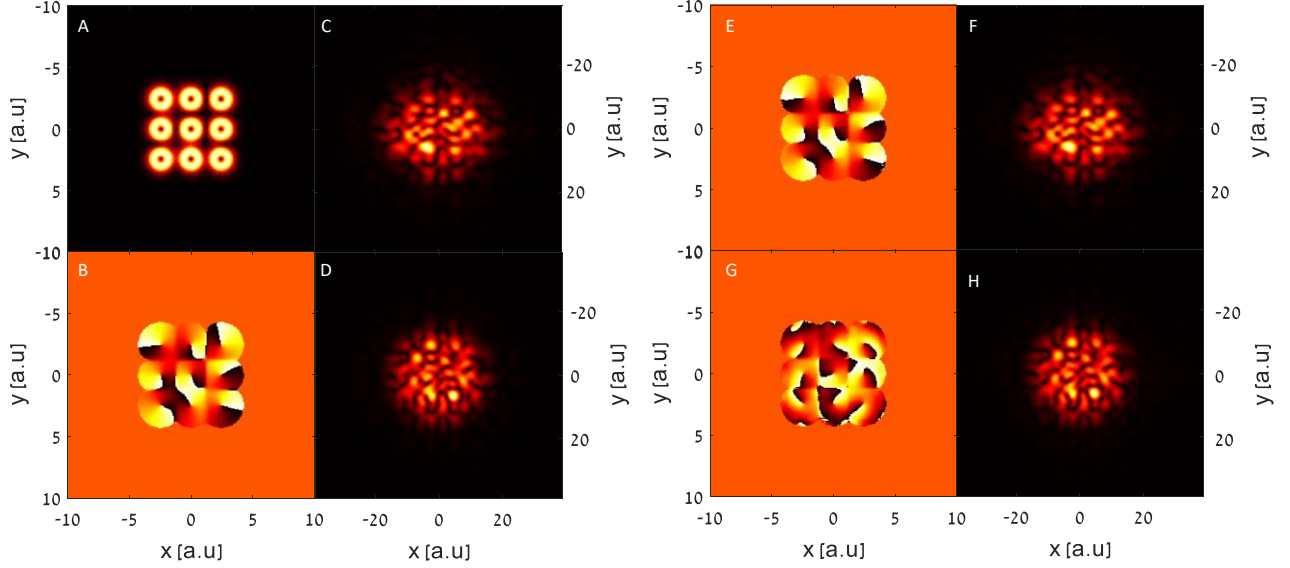


**Fig 5.** (A) Amplitude of wavefunction for reconstruction and (B) its phase, (C) is the augmented TOF and (D) is the original TOF. In (E), we can see phase reconstruction with the augmented TOF and its corresponding augmented TOF (F). In (G), an erroneous phase reconstruction from the original TOF and its corresponding original TOF (H), giving the same measurement but wrong object phase.

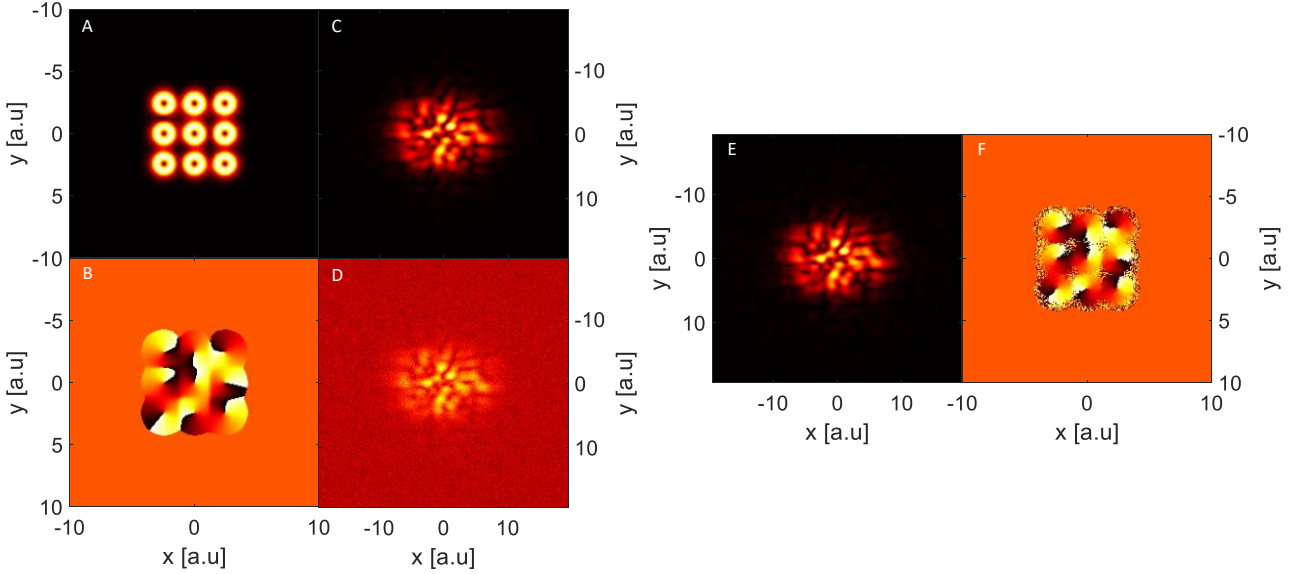


**Fig 6.** (A,B) Amplitude and phase of the reconstructed wavefunction, respectively. (C,D) Calculated atom density corresponding to augmented TOF measurement of (A,B), without appreciable noise and with added gaussian white noise, respectively. The noise in (D) is very strong, corresponding to SNR 0, yet the measurement scheme and the algorithm facilitate correct reconstruction, amplitude and phase, as shown in (E) and (F), respectively.

#### 4 Phase-retrieval of each measurement or of the expectation value?

Before closing, we wish to discuss the concept of phase retrieval in the context of experimental observables in quantum mechanics. Fundamentally, the wavefunction  $\psi(\mathbf{r}, t)$  is a probability amplitude, and its experimental observable is an expectation value, expressed as  $\langle |\psi(\mathbf{r}, t)|^2 \rangle$ , where the  $\langle \dots \rangle$  denotes ensemble averaging. Likewise, all experimental



observables of any quantum problem are expectation values expressed as projections on some set of functions defined by the measurement apparatus. In coming to perform phase-retrieval, this immediately raises a profound question deeply rooted in the foundations of quantum mechanics: should the phase-retrieval algorithm be performed on each individual measurement or on the ensemble-average?

In addressing this question, it is helpful to understand the phase-retrieval process as arising from reciprocity: phase-retrieval can be employed only on reciprocal problems because the concept relies on iterations between far-field (or TOF) measurements and constraints in the original "near-field" plane, such as the support. Obviously, the Schrödinger equation (Eq. 1) is reciprocal: taking  $t \rightarrow -t$  reverses the problem, and every process can be run backwards. However, ensemble averaging is not reciprocal; hence the answer should be that the phase-retrieval algorithm should be applied to each measurement in the ensemble and not on the ensemble-average, which is not reciprocal.

Let us explain this through the example given in Fig. 1. Obtaining high-quality experimental TOF data requires repeating the experiment multiple times, recording a set of TOF data  $|\psi_j(\mathbf{r}, T)|^2$ , with  $j = 1, 2, \dots, N$ , where  $N$  is the number of measurements (with the same initial wavefunction  $\psi_j(\mathbf{r}, t=0) = \psi(\mathbf{r}, t=0) \forall j$ ), and taking the ensemble average  $\langle |\psi(\mathbf{r}, t)|^2 \rangle$ . Attempting to retrieve the phase of the ensemble-average fails because each realization  $j$  also has its own global phase, which the algorithm cannot recover. Hence, the phase-retrieval procedure should be carried out separately for each realization  $|\psi_j(\mathbf{r}, T)|^2$ .

It is helpful to understand this issue through another quantum process known as Anderson localization, where it is known that every one-dimensional or two-dimensional disordered system leads to localization, and all transport comes to a complete halt[40]. This means that any set of arbitrary wavefunctions  $\psi_j(\mathbf{r}, t=0)$  which may be different from one another at  $t=0$  will lead to the same localized observable  $\langle |\psi(\mathbf{r}, t)|^2 \rangle$  after a long enough time  $T$ . Once again, keeping in mind that the Schrödinger equation is reciprocal, this raises a fundamental question: if we run the process backwards and launch the localized observable back in time, which of the initial wavefunction would we recover? The answer is that the ensemble-averaged observable is not reciprocal. Reciprocity means that launching  $\psi_j(\mathbf{r}, T)$  backwards indeed recovers each individual  $\psi_j(\mathbf{r}, t=0)$ , but to do that, one would need to know  $\psi_j(\mathbf{r}, T)$ , amplitude and phase, and not just  $\langle |\psi(\mathbf{r}, t)|^2 \rangle$ .

The understanding that phase-retrieval of the quantum wavefunction of BECs requires performing the algorithm on each experiment naturally raises some additional SNR issues, but these are not excessive as long as the number of atoms in the condensate is sufficiently large.

## 5 Discussion and Outlook

Our results show that the problem of reconstructing the phase of a BEC from TOF measurements is analogous to the phase retrieval problem in optics, with the distinction that the evolution of a BEC is nonlinear. We have shown that vortices and periodic arrays of vortices pose a problem that phase-retrieval (linear and nonlinear) from TOF (or far-field) measurements cannot resolve due to ambiguities. We have solved this ambiguity problem through an easily implemented augmentation of the measurement protocol of a BEC by a two-stage procedure: the trap is opened first in one direction and only after some time in the other direction. This procedure removes the ambiguities and, together with the proper phase-retrieval algorithm for nonlinear evolution, facilitates the correct recovery of complex quantum wavefunctions containing vortices and lattices of vortices. As vortices are a ubiquitous phenomenon with important implications for quantum technology and basic science, their correct reconstruction – including their helicity (topological charge) is crucial.

We analytically found the optimal propagation time under the partial trap for maximizing the measurement difference in the case of linear propagation and a single vortex and related it to the energy difference between the modes of the trap. In the context of measurement design, one possible future direction can be potential engineering. That is, instead of turning off the trap in stages in separate axes, engineering a time-dependent potential that will optimize signal recovery for specific classes of wavefunctions.

On the algorithmic side, the proof of concept we proposed utilized a basic iterative Fineup-type algorithm and shows there is sufficient information in the measurement for reconstruction in the cases we examined. While not pursued in this work, more advanced and novel algorithms can be adapted to the case of the BEC (especially the nonlinear propagation) to allow more robust recovery in the presence of noise.

We would like to emphasize that the only assumption of our method is that the **propagation** of the state follows the GPE, i.e., the mean-field approximation. This means that the evolution under the full trap does not strictly need to follow the GPE model; only the propagation of the measurement must follow the GPE. This point also hints at a future direction of incorporating more complex and advanced models into the retrieval problem, such as the Bogoliubov approximation [41], and extending this idea to Fermi gases as well.

Last but not least, we note that thus far, algorithmic phase-retrieval of the quantum wavefunctions of cold atoms has never been demonstrated in experiments. We are now pursuing this concept with an experimental group. Clearly, succeeding in recovering the quantum wavefunction from TOF measurements will revolutionize experimental techniques with cold atoms and will also apply to cold molecules[42], removing the excessively hard requirement for atom interference for unravelling the phase.

## Acknowledgements

## References

- [1] A. Einstein, "Zur Quantentheorie des idealen Gases," in *Albert Einstein: Akademie-Vorträge*, John Wiley & Sons, Ltd, 2005, pp. 258–266. doi: 10.1002/3527608958.ch29.
- [2] K. B. Davis *et al.*, "Bose-Einstein condensation in a gas of sodium atoms," *Physical review letters*, vol. 75, no. 22, p. 3969, 1995.
- [3] M. H. Anderson, J. R. Ensher, M. R. Matthews, C. E. Wieman, and E. A. Cornell, "Observation of Bose-Einstein condensation in a dilute atomic vapor," *science*, vol. 269, no. 5221, pp. 198–201, 1995.
- [4] D. W. Snoke, N. P. Proukakis, T. Giamarchi, and P. B. Littlewood, "Universality and Bose–Einstein condensation: Perspectives on recent work," *Universal Themes of Bose–Einstein Condensation*, 2017.
- [5] W. Ketterle, D. S. Durfee, and D. M. Stamper-Kurn, "Making, probing and understanding Bose-Einstein condensates," *arXiv:cond-mat/9904034*, Apr. 1999, Accessed: Sep. 08, 2021. [Online]. Available: <http://arxiv.org/abs/cond-mat/9904034>
- [6] M. R. Andrews, C. G. Townsend, H.-J. Miesner, D. S. Durfee, D. M. Kurn, and W. Ketterle, "Observation of interference between two Bose condensates," *Science*, vol. 275, no. 5300, pp. 637–641, 1997.
- [7] E. W. Hagley *et al.*, "Measurement of the coherence of a Bose-Einstein condensate," *Physical Review Letters*, vol. 83, no. 16, p. 3112, 1999.
- [8] M. E. Zawadzki, P. F. Griffin, E. Riis, and A. S. Arnold, "Spatial interference from well-separated split condensates," *Physical Review A*, vol. 81, no. 4, p. 043608, 2010.
- [9] Y. Torii *et al.*, "Mach-Zehnder Bragg interferometer for a Bose-Einstein condensate," *Phys. Rev. A*, vol. 61, no. 4, p. 041602, Feb. 2000, doi: 10.1103/PhysRevA.61.041602.
- [10] R. Ziv, Y. Sagi, Y. C. Eldar, and M. Segev, "Phase Retrieval of Vortices in Bose-Einstein Condensates," in *2021 Conference on Lasers and Electro-Optics (CLEO)*, 2021, pp. 1–2.
- [11] Y. Shechtman, Y. C. Eldar, O. Cohen, H. N. Chapman, J. Miao, and M. Segev, "Phase retrieval with application to optical imaging: a contemporary overview," *IEEE signal processing magazine*, vol. 32, no. 3, pp. 87–109, 2015.
- [12] J. R. Fienup, "Reconstruction of an object from the modulus of its Fourier transform," *Optics letters*, vol. 3, no. 1, pp. 27–29, 1978.
- [13] T. Bendory, R. Beinert, and Y. C. Eldar, "Fourier phase retrieval: Uniqueness and algorithms," in *Compressed Sensing and its Applications*, Springer, 2017, pp. 55–91.
- [14] Y. Shechtman, A. Beck, and Y. C. Eldar, "GESPAR: Efficient phase retrieval of sparse signals," *IEEE transactions on signal processing*, vol. 62, no. 4, pp. 928–938, 2014.
- [15] G. Wang, G. B. Giannakis, and Y. C. Eldar, "Solving systems of random quadratic equations via truncated amplitude flow," *IEEE Transactions on Information Theory*, vol. 64, no. 2, pp. 773–794, 2017.

- [16] G. Wang, L. Zhang, G. B. Giannakis, M. Akçakaya, and J. Chen, "Sparse phase retrieval via truncated amplitude flow," *IEEE Transactions on Signal Processing*, vol. 66, no. 2, pp. 479–491, 2017.
- [17] P. Schniter and S. Rangan, "Compressive phase retrieval via generalized approximate message passing," *IEEE Transactions on Signal Processing*, vol. 63, no. 4, pp. 1043–1055, 2014.
- [18] T. Bendory, D. Edidin, and Y. C. Eldar, "On signal reconstruction from FROG measurements," *Applied and Computational Harmonic Analysis*, vol. 48, no. 3, pp. 1030–1044, 2020.
- [19] T. Bendory, Y. C. Eldar, and N. Boumal, "Non-convex phase retrieval from STFT measurements," *IEEE Transactions on Information Theory*, vol. 64, no. 1, pp. 467–484, 2017.
- [20] K. Huang, Y. C. Eldar, and N. D. Sidiropoulos, "Phase retrieval from 1D Fourier measurements: Convexity, uniqueness, and algorithms," *IEEE Transactions on Signal Processing*, vol. 64, no. 23, pp. 6105–6117, 2016.
- [21] K. Jaganathan, Y. C. Eldar, and B. Hassibi, "STFT phase retrieval: Uniqueness guarantees and recovery algorithms," *IEEE Journal of selected topics in signal processing*, vol. 10, no. 4, pp. 770–781, 2016.
- [22] A. Kosior and K. Sacha, "Condensate Phase Microscopy," *Phys. Rev. Lett.*, vol. 112, no. 4, p. 045302, Jan. 2014, doi: 10.1103/PhysRevLett.112.045302.
- [23] D. Meiser and P. Meystre, "Reconstruction of the phase of matter-wave fields using a momentum-resolved cross-correlation technique," *Phys. Rev. A*, vol. 72, no. 2, p. 023605, Aug. 2005, doi: 10.1103/PhysRevA.72.023605.
- [24] M. R. Matthews, B. P. Anderson, P. C. Haljan, D. S. Hall, C. E. Wieman, and E. A. Cornell, "Vortices in a Bose-Einstein Condensate," *PHYSICAL REVIEW LETTERS*, vol. 83, no. 13, p. 4, 1999.
- [25] J. R. Abo-Shaer, C. Raman, J. M. Vogels, and W. Ketterle, "Observation of Vortex Lattices in Bose-Einstein Condensates," *Science*, Apr. 2001, Accessed: Sep. 08, 2021. [Online]. Available: <https://www.science.org/doi/abs/10.1126/science.1060182>
- [26] C. Lobo, A. Sinatra, and Y. Castin, "Vortex lattice formation in Bose-Einstein condensates," *Physical review letters*, vol. 92, no. 2, p. 020403, 2004.
- [27] D. V. Freilich, D. M. Bianchi, A. M. Kaufman, T. K. Langin, and D. S. Hall, "Real-Time Dynamics of Single Vortex Lines and Vortex Dipoles in a Bose-Einstein Condensate," *Science*, vol. 329, no. 5996, pp. 1182–1185, Sep. 2010, doi: 10.1126/science.1191224.
- [28] K. T. Kapale and J. P. Dowling, "Vortex Phase Qubit: Generating Arbitrary, Counterrotating, Coherent Superpositions in Bose-Einstein Condensates via Optical Angular Momentum Beams," *Phys. Rev. Lett.*, vol. 95, no. 17, p. 173601, Oct. 2005, doi: 10.1103/PhysRevLett.95.173601.
- [29] B. P. Anderson *et al.*, "Watching Dark Solitons Decay into Vortex Rings in a Bose-Einstein Condensate," *Phys. Rev. Lett.*, vol. 86, no. 14, pp. 2926–2929, Apr. 2001, doi: 10.1103/PhysRevLett.86.2926.
- [30] N. S. Ginsberg, J. Brand, and L. V. Hau, "Observation of Hybrid Soliton Vortex-Ring Structures in Bose-Einstein Condensates," *Phys. Rev. Lett.*, vol. 94, no. 4, p. 040403, Jan. 2005, doi: 10.1103/PhysRevLett.94.040403.
- [31] S. Burger *et al.*, "Dark Solitons in Bose-Einstein Condensates," *Phys. Rev. Lett.*, vol. 83, no. 25, pp. 5198–5201, Dec. 1999, doi: 10.1103/PhysRevLett.83.5198.
- [32] C.-A. Chen and C.-L. Hung, "Observation of Universal Quench Dynamics and Townes Soliton Formation from Modulational Instability in Two-Dimensional Bose Gases," *Phys. Rev. Lett.*, vol. 125, no. 25, p. 250401, Dec. 2020, doi: 10.1103/PhysRevLett.125.250401.
- [33] F. Dalfovo, S. Giorgini, L. P. Pitaevskii, and S. Stringari, "Theory of Bose-Einstein condensation in trapped gases," *Rev. Mod. Phys.*, vol. 71, no. 3, pp. 463–512, Apr. 1999, doi: 10.1103/RevModPhys.71.463.
- [34] C. J. Pethick and H. Smith, *Bose-Einstein condensation in dilute gases*. Cambridge university press, 2008.
- [35] A. V. Oppenheim and J. S. Lim, "The importance of phase in signals," *Proceedings of the IEEE*, vol. 69, no. 5, pp. 529–541, 1981.
- [36] S. Marchesini, "Invited Article: A unified evaluation of iterative projection algorithms for phase retrieval," *Review of Scientific Instruments*, vol. 78, no. 1, p. 011301, Jan. 2007, doi: 10.1063/1.2403783.
- [37] C.-H. Lu, C. Barsi, M. O. Williams, J. N. Kutz, and J. W. Fleischer, "Phase retrieval using nonlinear diversity," *Applied optics*, vol. 52, no. 10, pp. D92–D96, 2013.

- [38] S. Asokan, P. A. Yasir, and J. S. Ivan, "Estimation of dislocated phases in wavefronts through intensity measurements using a Gerchberg–Saxton type algorithm," *Applied Optics*, vol. 59, no. 24, pp. 7225–7232, 2020.
- [39] J. W. Fleischer *et al.*, "Observation of Vortex-Ring ``Discrete'' Solitons in 2D Photonic Lattices," *Phys. Rev. Lett.*, vol. 92, no. 12, p. 123904, Mar. 2004, doi: 10.1103/PhysRevLett.92.123904.
- [40] P. W. Anderson, "Absence of Diffusion in Certain Random Lattices," *Phys. Rev.*, vol. 109, no. 5, pp. 1492–1505, Mar. 1958, doi: 10.1103/PhysRev.109.1492.
- [41] N. P. Proukakis and B. Jackson, "Finite-temperature models of Bose–Einstein condensation," *J. Phys. B: At. Mol. Opt. Phys.*, vol. 41, no. 20, p. 203002, Oct. 2008, doi: 10.1088/0953-4075/41/20/203002.
- [42] A. Luski *et al.*, "Vortex beams of atoms and molecules," *Science*, vol. 373, no. 6559, pp. 1105–1109, Sep. 2021, doi: 10.1126/science.abj2451.

## Supplementary material A – Optimal Propagation Time Under Partial Trap

We wish to solve the following problem and find the optimal  $T_1$  parameter maximizing the difference between the magnitude of the  $\pm 1$  vortex states after propagation in our measurement scheme:

$$\max_{T_1} \left\| \left| \psi_1(x, y, T_1 + T_2) \right|^2 - \left| \psi_{-1}(x, y, T_1 + T_2) \right|^2 \right\|_2^2$$

We consider three Hamiltonians relating to the three stages of the augmented TOF measurement in the linear regime.  $H_0$  the Hamiltonian during complete trapping of the condensate,  $H_1$  after opening one axis of the trap and  $H_2$  the Hamiltonian of free propagation:

$$H_0 = \frac{P^2}{2m} + V(x, y) \quad H_1 = \frac{P^2}{2m} + V(x) \quad H_2 = \frac{P^2}{2m}$$

Let us take a symmetric separable potential. Since the potential is separable the solution is separable as well[1] and the eigen basis for the x and y dimensions is the same due to the symmetry of the Hamiltonian. A vortex mode is then given by:

$$\Psi_{\pm 1} = u_0(x)u_1(y) \pm iu_1(x)u_0(y)$$

where  $u_i(\cdot)$  is the i-th eigenfunction of the one-dimensional Hamiltonian,  $(\cdot)$  indicates the dependence on the dimension coordinate ( $x/y$  in our case). If we lift the potential barrier in one direction, the eigenfunction basis in that direction changes to that of a plane wave. We have:

$$u_i(\cdot) = \int_{-\infty}^{\infty} \langle k, u_i | k \rangle dk = \int_{-\infty}^{\infty} e^{ik(\cdot)} dk \int_{-\infty}^{\infty} u_i(\cdot) e^{-ik(\cdot)} d(\cdot)$$

which is the Fourier basis. Propagation in time is given by (for brevity  $\hbar$  is omitted and we implicitly divide and rescale our Hamiltonians by  $\hbar$ ):

$$\Psi(x, y, t_0 + T) = e^{-iH_1 T} \Psi(x, y, t_0)$$

If the wavefunction is an eigenfunction with eigenvalue (energy) we have:

$$\Psi(x, y, t_0 + T) = e^{-iH_1 T} \Psi(x, y, t_0) = e^{-iE_1 T} \Psi(x, y, t_0)$$

Therefore:

$$\begin{aligned} e^{-iH_1 T_1} \Psi_{\pm 1} &= e^{-iH_1 T_1} (u_0(x)u_1(y) \pm iu_1(x)u_0(y)) \\ &= \left( e^{-iE_0 T_1} u_0(x) \int_{-\infty}^{\infty} e^{-i\frac{k^2}{2m} T_1} \langle k, u_1 | k \rangle dk \pm i e^{-iE_1 T_1} u_1(x) \int_{-\infty}^{\infty} e^{-i\frac{k^2}{2m} T_1} \langle k, u_0 | k \rangle dk \right) \\ &= \left( e^{-iE_0 T_1} u_0(x) \int_{-\infty}^{\infty} u_1^{\mathcal{F}}(k) e^{-i\frac{k^2}{2m} T_1} e^{iky} dk \pm i e^{-iE_1 T_1} u_1(x) \int_{-\infty}^{\infty} u_0^{\mathcal{F}}(k) e^{-i\frac{k^2}{2m} T_1} e^{iky} dk \right) \end{aligned}$$

Here,  $u_i^{\mathcal{F}}(k)$  represents the Fourier coefficient of the  $i$ -th eigenfunction.

After propagation, a time  $T_1$  under potential in one direction, we remove the second potential and get:

$$e^{-iH_2T_2}\Psi_{\pm 1} = \begin{pmatrix} e^{-iE_0T_1} \int_{-\infty}^{\infty} u_0^{\mathcal{F}}(k) e^{-i\frac{k^2}{2m}T_2} e^{ikx} dk \cdot \int_{-\infty}^{\infty} u_1^{\mathcal{F}}(k) e^{-i\frac{k^2}{2m}(T_1+T_2)} e^{iky} dk \\ \pm i e^{-iE_1T_1} \int_{-\infty}^{\infty} u_1^{\mathcal{F}}(k) e^{-i\frac{k^2}{2m}T_2} e^{ikx} dk \int_{-\infty}^{\infty} u_0^{\mathcal{F}}(k) e^{-i\frac{k^2}{2m}(T_1+T_2)} e^{iky} dk \end{pmatrix}$$

Substituting in for the norm difference we wish to evaluate:

$$\left| \left| |\Psi_1|^2 - |\Psi_{-1}|^2 \right| \right|$$

We get:

$$\left| \left| |\Psi_1|^2 - |\Psi_{-1}|^2 \right| \right| = \left| \left| \begin{aligned} & \left| e^{-iE_0T_1} \int_{-\infty}^{\infty} u_0^{\mathcal{F}}(k) e^{-i\frac{k^2}{2m}T_2} e^{ikx} dk \cdot \int_{-\infty}^{\infty} u_1^{\mathcal{F}}(k) e^{-i\frac{k^2}{2m}(T_1+T_2)} e^{iky} dk \right. \\ & \left. + i e^{-iE_1T_1} \int_{-\infty}^{\infty} u_1^{\mathcal{F}}(k) e^{-i\frac{k^2}{2m}T_2} e^{ikx} dk \int_{-\infty}^{\infty} u_0^{\mathcal{F}}(k) e^{-i\frac{k^2}{2m}(T_1+T_2)} e^{iky} dk \right| \\ & - \left| e^{-iE_0T_1} \int_{-\infty}^{\infty} u_0^{\mathcal{F}}(k) e^{-i\frac{k^2}{2m}T_2} e^{ikx} dk \cdot \int_{-\infty}^{\infty} u_1^{\mathcal{F}}(k) e^{-i\frac{k^2}{2m}(T_1+T_2)} e^{iky} dk \right. \\ & \left. - i e^{-iE_1T_1} \int_{-\infty}^{\infty} u_1^{\mathcal{F}}(k) e^{-i\frac{k^2}{2m}T_2} e^{ikx} dk \int_{-\infty}^{\infty} u_0^{\mathcal{F}}(k) e^{-i\frac{k^2}{2m}(T_1+T_2)} e^{iky} dk \right| \end{aligned} \right|^2 \right|$$

In order to evaluate the integral, we will approximate its value using the stationary phase approximation[2]:

$$\int_{-\infty}^{\infty} u_i^{\mathcal{F}}(k) e^{-i\frac{k^2}{2m}T_2} e^{ik(\cdot)} dk \approx u_i^{\mathcal{F}} \left( \frac{m(\cdot)}{T_2} \right) e^{i\frac{m(\cdot)^2}{2T_2}} \int_{-\infty}^{\infty} e^{-i\frac{T_2}{2m} \left( k - \frac{m(\cdot)}{T_2} \right)^2} dk = u_i^{\mathcal{F}} \left( \frac{m(\cdot)}{T_2} \right) e^{i\frac{m(\cdot)^2}{2T_2}} \sqrt{-\frac{2\pi mi}{T_2}}$$

Substituting this into the previous equation:

$$\left| \left| |\Psi_1|^2 - |\Psi_{-1}|^2 \right| \right| = \left| \left| \begin{aligned} & \left| e^{-iE_0T_1} u_0^{\mathcal{F}} \left( \frac{mx}{T_2} \right) e^{i\frac{mx^2}{2T_2}} \sqrt{-\frac{2\pi mi}{T_2}} \cdot u_1^{\mathcal{F}} \left( \frac{my}{(T_1+T_2)} \right) e^{i\frac{my^2}{2(T_1+T_2)}} \sqrt{-\frac{2\pi mi}{(T_1+T_2)}} \right. \\ & \left. + i e^{-iE_1T_1} u_1^{\mathcal{F}} \left( \frac{mx}{T_2} \right) e^{i\frac{mx^2}{2T_2}} \sqrt{-\frac{2\pi mi}{T_2}} u_0^{\mathcal{F}} \left( \frac{my}{(T_1+T_2)} \right) e^{i\frac{my^2}{2(T_1+T_2)}} \sqrt{-\frac{2\pi mi}{(T_1+T_2)}} \right| \\ & - \left| e^{-iE_0T_1} u_0^{\mathcal{F}} \left( \frac{mx}{T_2} \right) e^{i\frac{mx^2}{2T_2}} \sqrt{-\frac{2\pi mi}{T_2}} \cdot u_1^{\mathcal{F}} \left( \frac{my}{(T_1+T_2)} \right) e^{i\frac{my^2}{2(T_1+T_2)}} \sqrt{-\frac{2\pi mi}{(T_1+T_2)}} \right. \\ & \left. - i e^{-iE_1T_1} u_1^{\mathcal{F}} \left( \frac{mx}{T_2} \right) e^{i\frac{mx^2}{2T_2}} \sqrt{-\frac{2\pi mi}{T_2}} u_0^{\mathcal{F}} \left( \frac{my}{(T_1+T_2)} \right) e^{i\frac{my^2}{2(T_1+T_2)}} \sqrt{-\frac{2\pi mi}{(T_1+T_2)}} \right| \end{aligned} \right|^2 \right|$$

Removing the common phase term and taking the common factor outside of the norm operation yields:

$$= \frac{2\pi m}{\sqrt{T_2(T_1+T_2)}} \left\| \left| -e^{-iE_0T_1} u_0^{\mathcal{F}} \left( \frac{mx}{T_2} \right) \cdot u_1^{\mathcal{F}} \left( \frac{my}{(T_1+T_2)} \right) i + e^{-iE_1T_1} u_1^{\mathcal{F}} \left( \frac{mx}{T_2} \right) u_0^{\mathcal{F}} \left( \frac{my}{(T_1+T_2)} \right) \right|^2 \right. \\ \left. - \left| e^{-iE_0T_1} u_0^{\mathcal{F}} \left( \frac{mx}{T_2} \right) \cdot u_1^{\mathcal{F}} \left( \frac{my}{(T_1+T_2)} \right) i + e^{-iE_1T_1} u_1^{\mathcal{F}} \left( \frac{mx}{T_2} \right) u_0^{\mathcal{F}} \left( \frac{my}{(T_1+T_2)} \right) \right|^2 \right\|$$

We note that the eigen wavefunctions can be taken to be real, and by the properties of bounded eigen wavefunctions in symmetric potentials, the ground state is even and the first excited is odd. Therefore, by the Fourier properties, in the Fourier plane  $u_0^{\mathcal{F}}(\cdot)$  is a real and even function and  $u_1^{\mathcal{F}}(\cdot)$  is an imaginary and even function. Therefore:

$$\frac{2\pi m}{\sqrt{T_2(T_1+T_2)}} \left\| \left| u_0^{\mathcal{F}} \left( \frac{mx}{T_2} \right) \cdot u_1^{\mathcal{F}} \left( \frac{my}{(T_1+T_2)} \right) + u_1^{\mathcal{F}} \left( \frac{mx}{T_2} \right) u_0^{\mathcal{F}} \left( \frac{my}{(T_1+T_2)} \right) (i \cos(\Delta ET_1) + \sin(\Delta ET_1)) \right|^2 \right. \\ \left. - \left| -u_0^{\mathcal{F}} \left( \frac{mx}{T_2} \right) \cdot u_1^{\mathcal{F}} \left( \frac{my}{(T_1+T_2)} \right) + u_1^{\mathcal{F}} \left( \frac{mx}{T_2} \right) u_0^{\mathcal{F}} \left( \frac{my}{(T_1+T_2)} \right) (i \cos(\Delta ET_1) + \sin(\Delta ET_1)) \right|^2 \right\|$$

By the absolute value operation:

$$= \frac{2\pi m}{\sqrt{T_2(T_1+T_2)}} \left\| \left( \left( u_0^{\mathcal{F}} \left( \frac{mx}{T_2} \right) \cdot u_1^{\mathcal{F}} \left( \frac{my}{(T_1+T_2)} \right) + u_1^{\mathcal{F}} \left( \frac{mx}{T_2} \right) u_0^{\mathcal{F}} \left( \frac{my}{(T_1+T_2)} \right) \sin(\Delta ET_1) \right)^2 \right. \right. \\ \left. \left. + \left( u_1^{\mathcal{F}} \left( \frac{mx}{T_2} \right) u_0^{\mathcal{F}} \left( \frac{my}{(T_1+T_2)} \right) \cos(\Delta ET_1) \right)^2 \right) \right. \\ \left. - \left( \left( u_0^{\mathcal{F}} \left( \frac{mx}{T_2} \right) \cdot u_1^{\mathcal{F}} \left( \frac{my}{(T_1+T_2)} \right) - u_1^{\mathcal{F}} \left( \frac{mx}{T_2} \right) u_0^{\mathcal{F}} \left( \frac{my}{(T_1+T_2)} \right) \sin(\Delta ET_1) \right)^2 \right) \right. \\ \left. \left. + \left( u_1^{\mathcal{F}} \left( \frac{mx}{T_2} \right) u_0^{\mathcal{F}} \left( \frac{my}{(T_1+T_2)} \right) \cos(\Delta ET_1) \right)^2 \right) \right\|$$

Simplifying:

$$= \frac{2\pi m}{\sqrt{T_2(T_1+T_2)}} \left\| \left( u_0^{\mathcal{F}} \left( \frac{mx}{T_2} \right) \cdot u_1^{\mathcal{F}} \left( \frac{my}{(T_1+T_2)} \right) + u_1^{\mathcal{F}} \left( \frac{mx}{T_2} \right) u_0^{\mathcal{F}} \left( \frac{my}{(T_1+T_2)} \right) \sin(\Delta ET_1) \right)^2 \right. \\ \left. - \left( u_0^{\mathcal{F}} \left( \frac{mx}{T_2} \right) \cdot u_1^{\mathcal{F}} \left( \frac{my}{(T_1+T_2)} \right) - u_1^{\mathcal{F}} \left( \frac{mx}{T_2} \right) u_0^{\mathcal{F}} \left( \frac{my}{(T_1+T_2)} \right) \sin(\Delta ET_1) \right)^2 \right\|$$

$$= \frac{2\pi m}{\sqrt{T_2(T_1+T_2)}} \left\| 4u_0^{\mathcal{F}}\left(\frac{mx}{T_2}\right) \cdot u_1^{\mathcal{F}}\left(\frac{my}{(T_1+T_2)}\right) \cdot u_1^{\mathcal{F}}\left(\frac{mx}{T_2}\right) u_0^{\mathcal{F}}\left(\frac{my}{(T_1+T_2)}\right) \sin(\Delta ET_1) \right\|$$

Finally, we find:

$$\left| \|\psi_1\|^2 - \|\psi_{-1}\|^2 \right| = \frac{2\pi m}{\sqrt{T_2(T_1+T_2)}} \left\| 4u_0^{\mathcal{F}}\left(\frac{mx}{T_2}\right) \cdot u_1^{\mathcal{F}}\left(\frac{my}{(T_1+T_2)}\right) \cdot u_1^{\mathcal{F}}\left(\frac{mx}{T_2}\right) u_0^{\mathcal{F}}\left(\frac{my}{(T_1+T_2)}\right) \sin(\Delta ET_1) \right\|$$

We can see the magnitude difference is proportional to  $\frac{\sin(\Delta ET_1)}{\sqrt{T_2(T_1+T_2)}}$  directly, with indirect dependence on  $T_1$

through the scaling of  $u_1^{\mathcal{F}}, u_0^{\mathcal{F}}$  in the norm operation. As the scaling is governed by  $T_2$ , which we assume to be larger than  $T_1$  in our setting, the overlap between the eigenfunctions in the norm operation has weak dependence on  $T_1$ . We conclude that:

$$\left| \|\psi_1\|^2 - \|\psi_{-1}\|^2 \right| \propto \frac{\sin(\Delta ET_1)}{\sqrt{T_2(T_1+T_2)}}$$

- [1] Eisenhart, L. P. "Enumeration of potentials for which one-particle Schrödinger equations are separable." *Physical Review* 74.1 (1948): 87.
- [2] Wong, Roderick. *Asymptotic approximations of integrals*. Society for Industrial and Applied Mathematics, 2001.



## Supplementary material B – Simulation details

In this section, we describe the simulation method and parameters used in the main text. We solve a dimensionless GPE:

$$\left( -\frac{\hbar^2}{2m} \nabla^2 + V(\mathbf{r}) + U_0 |\psi(\mathbf{r}, t)|^2 \right) \psi(\mathbf{r}, t) = i\hbar \partial_t \psi(\mathbf{r}, t)$$

where  $\hbar, m$  are taken to be unity. The potential is taken as a potential well with depth  $10[a.u]$  and radius 1. The nonlinear coefficient is chosen in the range  $U_0 \in [0, 100]$ . As the wavefunction is normalized to unity, it should be understood that this factor implicitly contains the total particle number inside the condensate, i.e.,  $U_0 = \frac{4\pi\hbar^2 a_s}{m} N_0$ , where  $N_0$  is the total particle number and  $a_s$  is the scattering length. We note that in Fig 2 and Fig 3,  $U_0$  is taken as 0 for linear propagation, 100 for weak nonlinearity, and 10000 for strong nonlinearity. These values are chosen such that  $V(\mathbf{r}) \gg U_0 |\psi(\mathbf{r}, t)|^2$  and  $U_0 |\psi(\mathbf{r}, t)|^2 \gg V(\mathbf{r})$ , for the last two cases, respectively.

The spatial dimensions are discretized into a  $1024 \times 1024$  grid with a resolution of  $dx = dy = 0.0756[a.u]$ . For propagation, we use the BPM or split-step method with a temporal step of  $dt = 10^{-3}$ . The number of steps for complete propagation in the TOF and augmented TOF is taken to be 3000. In the augmented TOF, the number of steps taken under the partial propagation is set to be 558 (corresponding to  $\frac{\Delta E T_1}{\hbar} = \pi/2$ , see section 3.3), while the rest of the propagation steps are done under free propagation with no potential. We note that, for the noise simulations the propagation time is taken to be slightly shorter in order to ease computation time over repeated runs, a total of 1500 steps with 558 being under the partial potential and the rest in free propagation.

The lattice is constructed by duplicating the well potential into a  $3 \times 3$  lattice with separation of  $\Delta x = \Delta y \approx 2.4$ . The vortex lattice wavefunction is constructed in a similar way, placing a single vortex at the center of each well potential with a random flow direction and relative phase to the other sites.